Electrochemical Preparation and Characterization of Meisenheimer Complexes of Trinitrofluorenone with Pyrrole, Indole, and Carbazole

Nobuo Ozawa,[†] Hiroko Seki,[‡] Takashi Kitamura,[†] Hiroshi Kokado,[†] Tsutomu Ishikawa,[§] and Katsuyoshi Hoshino*,[†]

Faculty of Engineering, Chemical Analysis Center, and Faculty of Pharmaceutical Sciences, Chiba University, 1-33 Yayoi, Inage, Chiba 263-8522, Japan

Received May 18, 2001. Revised Manuscript Received December 28, 2001

The mechanism of Meisenheimer complex formation by a novel electrochemical route was investigated. The synthetic route utilizes a CH_3CN solution consisting of trinitrofluorenone (TNF), electron-donative molecules (EDM = pyrrole, indole, and carbazole), and a supporting electrolyte. Electroreduction of the solution causes a complexation of TNF with the EDMs to yield a green anionic σ complex. To understand this electrode reaction, the effects of electrolysis and solution conditions (solvent, supporting electrolyte, the role of O_2, etc.) on the complex formation were investigated. As a result, it was revealed that the σ-complex formation proceeds in the following successive steps: (1) charge-transfer (CT) complex formation between TNF and the EDMs, (2) two-electron reduction of the CT complex to yield double-anionic radical species, (3) attack of O_2 on the radical species to induce complexation of TNF with the EDMs, and (4) stabilization of the resulting σ complex by hydrophobic electrolyte cations. In addition, kinetic and X-ray photoelectron spectroscopic measurements revealed that the σ complexes possess unique electronic structures with high stability (first-order decomposition rate constant of 2.3×10^{-6}−1.0×10^{-5} s^{-1} at 20 °C in acetone; no decomposition at 0 °C in the solid state and in acetone).

Introduction

Recently, we reported the first electrochemical synthesis of a Meisenheimer or anionic σ complex[1] (**4a**; Chart 1), which is formed between pyrrole (Py) and 2,4,7-trinitro-9-fluorenone (TNF), as an inseparable 9:2 isomeric mixture. Meisenheimer complexes are formed by the strong interaction of electron-deficient aromatics with nucleophiles[2] and are generally characterized by their intensely colored solutions and the involvement of an sp^3 carbon atom in their molecular structures. The complex **4a** is distinguished from most of the earlier complexes in that (1) it is the first to be prepared electrochemically, (2) its lifetime is long enough to be isolated, (3) a nonnucleophilic Py molecule contributes to the complex formation,[2c,3] (4) its constituents, Py and TNF, are technologically important molecules, with the former being chemically or electrochemically polymerized to give one of the best known conducting polymers (polypyrrole)[4] and the latter the best known electron-transporting material in electrophotography,[5] and (5) its electropolymerization forms a unique polypyrrole film that can be doped with both anionic (p-type doping) and cationic species (n-type doping).[6]

Chart 1

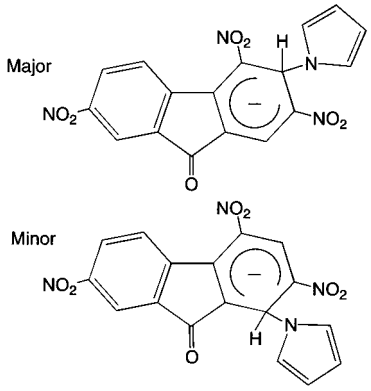

4a

* To whom correspondence should be addressed. E-mail: hoshino@image.tp.chiba-u.ac.jp.
† Faculty of Engineering.
‡ Chemical Analysis Center.
§ Faculty of Pharmaceutical Sciences.

(1) Hoshino, K.; Ozawa, N.; Kokado, H.; Seki, H.; Tokunaga, T.; Ishikawa, T. *J. Org. Chem.* **1999**, *64*, 4572 and 4573.

(2) (a) Jackson, C. F.; Gazzolo, F. H. *Am. Chem. J.* **1900**, *23*, 376−396. (b) Meisenheimer, J. *Justus Liebigs Ann. Chem.* **1902**, *323*, 205−246. (c) Terrier, F. *Chem. Rev.* **1982**, *82*, 77−152. (d) Strauss, M. J. *Chem. Rev.* **1970**, *70*, 667−712. (e) Artamkina, G. A.; Egorov, M. P.; Beletskaya, I. P. *Chem. Rev.* **1982**, *82*, 427−459. (f) Consiglio, G.; Spinelli, D.; Dell'Erba, C.; Novi, M.; Petrillo, G. *Gazz. Chim. Ital.* **1997**, *127*, 753−769. (g) Badea, F. *Reaction Mechanism in Organic Chemistry*; Abacus Press: Tunbridge Wells, Kent (England), 1974; pp 413−415. (h) Buncel, E.; Dust, J. M.; Terrier, F. *Chem. Rev.* **1995**, *95*, 2261−2280. (i) Terrier, F.; Sebban, M.; Goumont, R.; Halle, G.; Moutiers, G.; Cangelosi, I.; Buncel, E. *J. Org. Chem.* **2000**, *65*, 7391−7398 and references therein.

(3) The addition of pyrrolide or indolide ion to trinitrobenzene appeared as an almost unique example of the formation of a nitrogen-bonded σ complex: Halle, J. C.; Terrier, F.; Pouet, M. J.; Simonnin, M. P. *J. Chem. Res. (S)* **1980**, 360 and 361.

(4) (a) Diaz, A. F.; Kanazawa, K. K.; Gardini, G. P. *J. Chem. Soc., Chem. Commun.* **1979**, 635 and 636. (b) Kanazawa, K. K.; Diaz, A. F.; Geiss, R. H.; Gill, W. D.; Kwak, J. F.; Logan, J. A.; Rabolt, J. F.; Street, G. B. *J. Chem. Soc., Chem. Commun.* **1979**, 854 and 855.

(5) Gill, W. D. *J. Appl. Phys.* **1972**, *43*, 5033−5040.

10.1021/cm010488i CCC: $22.00
Published on Web 02/21/2002

Chart 2

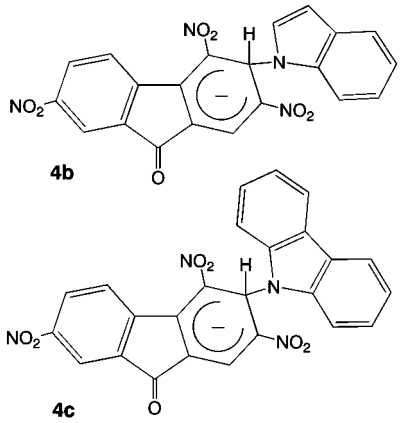

In our previous study,[1] the synthetic procedure and structural analyses of **4a** have been reported. However, little is known about its formation mechanism, physicochemical properties, and feasibility to use alternatives to Py, and hence its synthetic conditions have been optimized empirically in the potential application as a precursor of a new class of conducting polymeric materials. A knowledge of the mechanism should be a necessary requirement for designing such conducting materials and for establishing a theoretical description. In this paper, we report the results of a detailed study on the electrochemical formation of the complexes **4** by systematic variation of the preparation conditions. The formation is greatly affected by conditions such as the solvent, the supporting electrolyte, and the atmosphere during the electrolysis. This study is coupled with the evaluation of the complex properties and is extended to the elucidation of the complex-formation mechanism. The evaluation includes thermal stability by UV−vis absorption spectroscopy and electronic structures by X-ray photoelectron spectroscopy (XPS or ESCA). In addition, the similar complexation of TNF with indole (Ind) and carbazole (Cz) as in **4b** and **4c** is also described (Chart 2).

Experimental Section

Materials. Electron-donative molecules of reagent grade (abbreviated as EDM) Py, Ind, Cz, thiophene (Th), and 1-methylpyrrole (MePy) were obtained from Tokyo Kasei Kogyo Co. and employed for the reaction with TNF (Tokyo Kasei Kogyo Co.); they have been reported to be precursors for the chemical or electrochemical synthesis of conducting polymers.[7] Py and Th were purified by distillation just before use, with the others being used as supplied.

Cyclic Voltammetry. The cyclic voltammograms (CV)[8] of TNF in the presence or absence of an EDM were conducted in a two-compartment cell equipped with a platinum disk (working electrode; BAS Co.), platinum wire (counter electrode; Tanaka Kikinzoku Co.), and saturated calomel electrode (reference electrode abbreviated as SCE; TOA Co.) under a flow of N_2. Before use, the Pt disk with a geometric area of 0.021 cm^2 was polished on a felt disk with a 12.5 μm Al_2O_3 paste (Buehler) and ultrasonically washed with distilled deionized water, acetone, and tetrahydrofuran (THF). The solvents used were spectroscopic-grade CH_3CN, CH_2Cl_2, THF, and dimethylformamide (DMF; Kanto Chemical Co.). As the supporting electrolytes, reagent-grade $(C_2H_5)_4N^+ClO_4^-$ (TEAP), $(C_4H_9)_4N^+ClO_4^-$ (TBAP), $(C_4H_9)_4N^+BF_4^-$ (TBABF$_4$), $LiClO_4$, and $NaClO_4$ were used (Tokyo Kasei Kogyo Co.).

Scheme 1. Expected Reaction Scheme for the Electrochemical σ-Complex (4) Formation between EDM and TNF

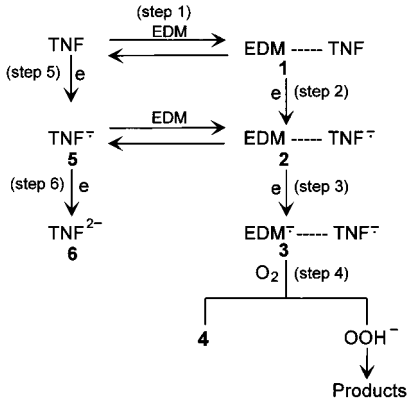

Electrochemical Synthesis. The electrochemical synthesis of **4a** has already been reported:[1] Controlled-potential electrolysis[9] of a CH_3CN solution containing Py (20 mM), TNF (20 mM), and TEAP (0.1 M) was done at −1.0 V vs SCE while stirring under ice cooling and a flow of N_2. A platinum gauze (3.5 cm × 12.5 cm, 55 mesh) in the main compartment and a platinum plate (3.0 × 2.5 cm^2) in the auxiliary compartment were used as the working and counter electrodes, respectively, which were separated from each other by a sintered glass frit. After the electrolysis, the color of the electrolyte solution turned from orange to green. Workup of it after treatment with sodium perchlorate gave the green powder of **4a** in 15% isolated yield.[10] Unless otherwise noted, solutions were purged with N_2 for 1 h prior to electrochemical measurements. The electrolysis cells were connected to a Hokuto Denko model HAB-151 potentiostat. The CV traces were recorded on a Riken Denshi model F-35A *xy* recorder.

UV−vis and XPSs. The UV−vis absorption spectra were recorded on a Shimazu UV-2100 spectrophotometer. For the XPS measurements, an ULVAC φ ESCA 5400 spectrometer with Mg Kα radiation was used. The absolute binding energy scale was obtained by setting the C 1s peak to 284.6 eV.

Results and Discussion

In our previous study,[1] a possible mechanism for the electrochemical formation of **4a** (Scheme 1) was proposed which involves the successive steps of charge-transfer (CT) or π-complex formation between EDM and TNF (**1**), electrochemical two-electron reduction of the complex to yield a double-anionic radical species (**3**), and reaction of O_2 with the radical species to form the σ complex (**4a**). In the following, we describe how experimental evidence, provided by UV−vis absorption, CV, and XPS measurements, rationalized the expected mechanism for the formation of **4**.

CT or π-Complex Formation (Step 1). The formation of **1** was monitored spectrophotometrically. Figure

(6) Details of the chemical, electrochemical, and electronic characterization of the new polypyrrole films will be reported elsewhere.

(7) Diaz, A. F.; Bargon, J. Electrochemical Synthesis of Conducting Polymers. In *Handbook of Conducting Polymers*; Skotheim, T. A., Ed.; Marcel Dekker: New York, 1986; Vol. 1, pp 81−115.

(8) Bard, A. J.; Faulkner, L. R. *Electrochemical Methods*; John Wiley & Sons: New York, 1980; Chapter 6, pp 213−248.

(9) See Chapter 10 (pp 370−428) in ref 8.

(10) In our previous study, we observed that a tetraethylammonium salt of **4a** was obtained by the electroreduction of the mixture in a TEAP/CH_3CN solution. However, the product tended to incorporate Na^+ during purification by column chromatography (SiO_2) using Wakogel C-100, which is known to contain a small amount of Na^+. This required posttreatment with sodium perchlorate in order to obtain a well-defined structure of **4a**.

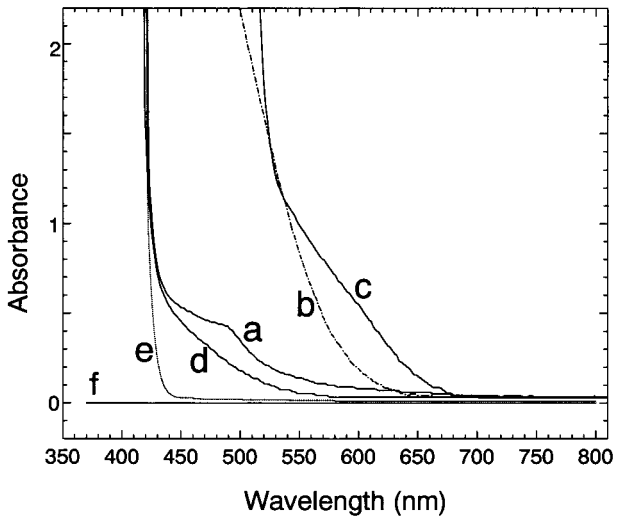

Figure 1. UV−vis absorption spectra of TNF (20 mM)/EDM (0.1 M) mixtures in CH_3CN at 20 °C: a, EDM = Py; b, Ind; c, Cz; d, MePy. The curves e and f show the spectra of CH_3CN solutions containing TNF (20 mM) and EDMs (0.1 M), respectively.

1 shows the UV−vis spectra of CH_3CN solutions containing TNF (20 mM) plus 0.1 M of Py (a), Ind (b), Cz (c), and MePy (d) at 20 °C. Included for comparison in this figure is the spectrum of TNF itself (20 mM; spectrum e). No absorption was exhibited by the EDMs in the visible region (spectrum f). The addition of MePy, Py, Ind, and Cz changed the color of the TNF solution from pale yellow to yellow, orange, red, and reddish brown, respectively: The intensity and absorption edge of the new band in the visible region increased in this order. In the cases of Ind and Cz, precipitation occurred on their addition to the TNF solution, so that the supernatant was used for their absorption measurements. Though not shown here, no change in spectrum e was observed when adding Th to the TNF solution. These observations show the formation of complex **1**, except for Th, and the increasing interaction in the order of MePy < Py < Ind < Cz.

Electroreduction of 1 (Steps 2 and 3). In Scheme 1, the interaction is assumed to play a crucial role in the formation of **4**. The role was therefore investigated by cyclic voltammetric measurements of the above solutions, and the mode of generation of **4** was observed. Figure 2 shows CVs for the reduction of TNF in the presence (solid curves) and absence of EDM (dotted curves): a, EDM = Py; b, Ind; c, Cz; d, Th; e, MePy. In this measurement also, the supernatant was employed in the cases of Ind and Cz, and therefore, their currents are somewhat smaller compared to that indicated by the corresponding dotted curve. The CV of TNF shows well-defined reversible waves with half-wave potentials of −0.49 (step 5 in Scheme 1) and −0.73 V vs SCE (step 6),[11] whereas no redox wave was observed in the voltammograms of EDMs in the potential range of 0 to −1.2 V (not shown here). The voltammetric wave of TNF was altered by the addition of Py, Ind, and Cz. The first (step 5) and second (step 6) reduction waves of TNF were also observed in the CVs a−c, but the latter is accompanied by a new wave identified as the electroreduction in step 3. The peak potentials of these new waves were −0.83, −0.80, and −0.77 V for Py, Ind, and Cz, respectively, the order of which is in agreement with that of CT interaction in the complex **1**, Py < Ind < Cz. The scan rate dependence of the waves for the Py−TNF solution indicated that they correspond to a thermodynamic equilibrium (see the Supporting Information). The facts that the green products **4** were formed near and below the second peak potentials and that no formation of **4** occurred under only a one-electron-reduction condition (−0.6 V, step 2) may be direct evidence for the identification. The complexes of **4a**−**c** have two maxima in the visible region (Table 1), and their spectra were quite similar in shape to those of trinitrocyclohexadienates (see Figure 3 and Table 9 in ref 2d): Calculation of UV−vis electronic spectra for the isomers of **4a** using a semiempirical quantum mechanical program (ZINDO) and their comparison with the measured spectra for **4a**−**c** suggests that **4b** and **4c**, like **4a**, are also the isomeric mixtures (the calculated and measured spectra are available in the Supporting Information). We previously speculated that the electronic structure of $TNF^{\cdot-}$ in the complex **2** is expected to be similar to that of TNF^{2-} because of the donation of electrons from EDM to $TNF^{\cdot-}$, and hence, the second electron would be transferred to the electron-deficient EDM to produce a double-radical anion **3**. If we assume that the order of CT interaction in complex **2** is the same as that in complex **1**, CT theory[12] predicts that the deficiency of electrons in the EDMs is in the order of the Cz > Ind > Py moiety in complex **2**, being in agreement with the order of ease with which they are reduced. On the other hand, in the CVs of d and e, the waves for the mixture of TNF and EDM (solid curves) were nearly the same in shape and position of the peaks as those for TNF (dotted curve). Additionally, the product in their controlled-potential electrolysis at −1.0 V was not complex **4** (green) but **6** (dull red). These results demonstrated that the CT interaction and the lack of N substitution are prerequisites for the electrosynthesis of complex **4**. Bunton et al. have shown that CT complexes are formed prior to the formation of the Meisenheimer complexes[13] and that the former complexes are also the intermediates in nucleophilic aromatic substitution reactions. Recently, Terrier et al. reported the first isolation of a CT-complex precursor in Meisenheimer complex formation.[14]

Table 1. Visible Absorption Maxima of 9-Oxo-2,4,7-trinitroindanyl[5,6-*b*]cyclohexadienates 4a−c in Acetone at 20 °C

complex	λ_{max} (nm)	complex	λ_{max} (nm)
4a	477, 611	**4c**	478, 612
4b	474, 611		

(11) Loutfy, R. O.; Hsiao, C. K.; Ong, B. S.; Keoshkerian, B. *Can. J. Chem.* **1984**, *62*, 1877−1885.

(12) (a) Mulliken, R. S. *J. Am. Chem. Soc.* **1952**, *74*, 811−824. (b) Tsubomura, H.; Mulliken, R. S. *J. Am. Chem. Soc.* **1960**, *82*, 5966−5974. (c) Mulliken, R. S. *J. Phys. Chem.* **1952**, *56*, 801−822.

(13) (a) Bacaloglu, R.; Bunton, C. A.; Cerichelli, G. *J. Am. Chem. Soc.* **1987**, *109*, 621−623. (b) Bacaloglu, R.; Blasko, A.; Bunton, C. A.; Dorwin, E.; Ortega, F.; Zucco, C. *J. Am. Chem. Soc.* **1991**, *113*, 238−246. (c) Bacaloglu, R.; Blasko, A.; Bunton, C. A.; Ortega, F.; Zucco, C. *J. Am. Chem. Soc.* **1992**, *114*, 7708−7718. (d) Bacaloglu, R.; Bunton, C. A.; Cerichelli, G.; Ortega, F. *J. Am. Chem. Soc.* **1988**, *110*, 3495−3503.

(14) Sepulcri, P.; Goumont, R.; Halle, J.-C.; Buncel, E.; Terrier, F. *Chem. Commun.* **1997**, 789 and 790.

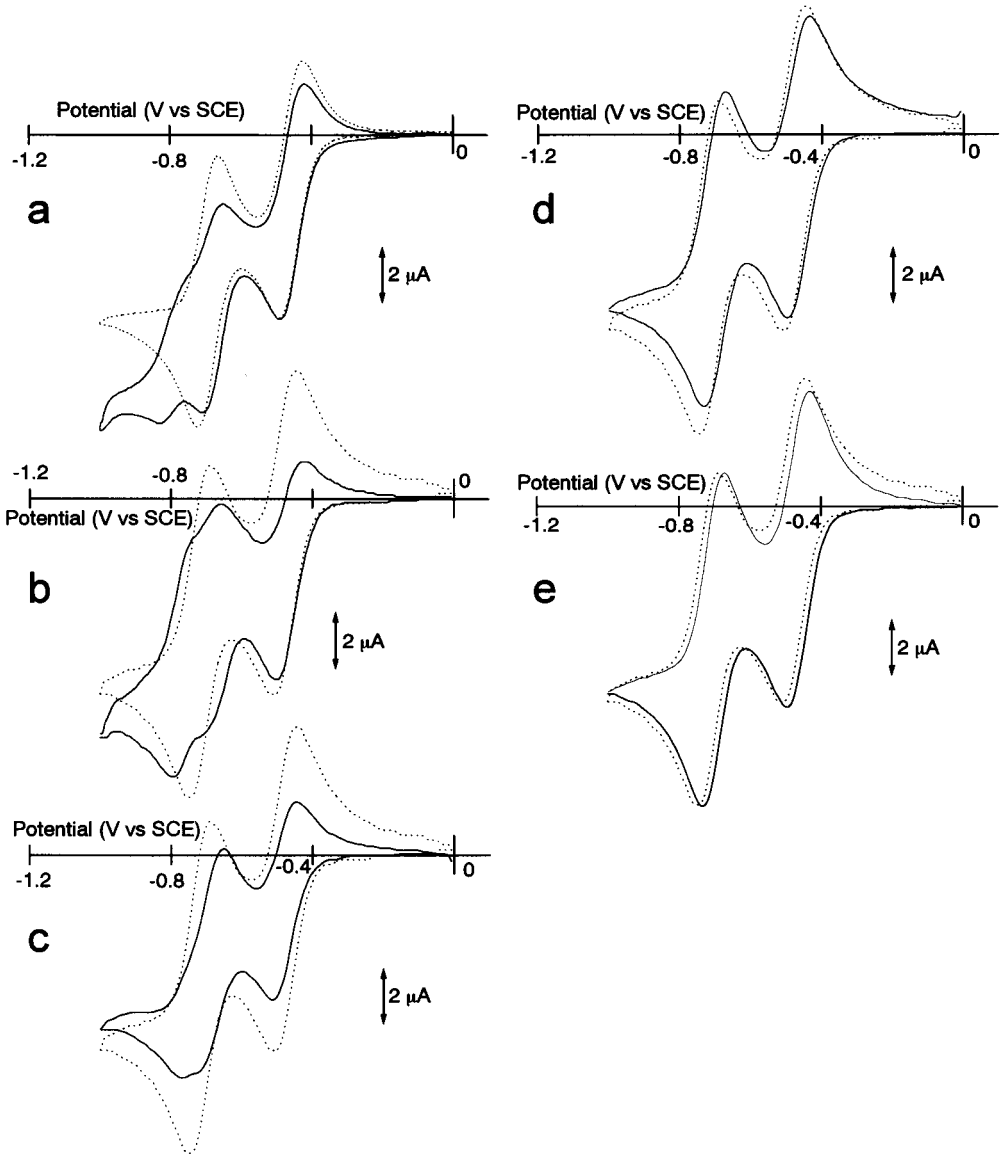

Figure 2. CVs of CH_3CN solutions containing TNF (2 mM), EDM (0.1 M), and TEAP (0.1 M) at 20 °C (solid curves). EDM: a, Py; b, Ind; c, Cz; d, Th; e, MePy. Dotted curves stand for the voltammograms of CH_3CN solutions containing TNF (2 mM) and TEAP (0.1 M). Sweep rate: 20 mV/s. Working electrode: Pt disk (0.021 cm^2).

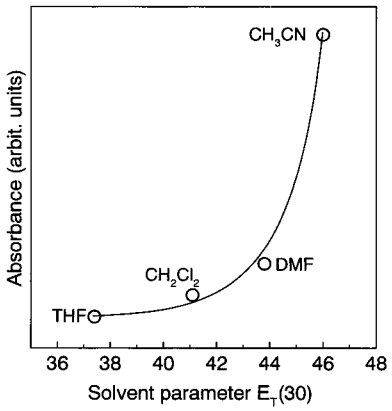

Figure 3. Relationship between the yield of complex **4a** and the solvent parameter $E_T(30)$. The absorbance of **4a** at λ_{max} = 611 nm was chosen as an indication of the yield. The electrolysis and solution conditions for the preparation of **4a** were described in the text.

Solvent Effect for the Formation of 4a. The equilibrium constant for the formation of the CT state (and accordingly its concentration) is expected to depend on the microscopic polarity of the surrounding solvent molecules. Thus, the effect of the solvent on the rate of production of **4a** was investigated. Controlled-potential electrolyses of solutions containing Py (0.1 M), TNF (0.02 M), and TBAP (0.1 M) were carried out in the four solvents described in the Experimental Section: working electrode, Pt plate (5.0 cm^2); reduction potential, −1.0 V vs SCE which is well below the potential for the formation of complex **4a** in each solvent; temperature, 0 °C; electrolysis time, 2 h. The resultant green solutions were then diluted and subjected to UV−vis absorption measurements. Figure 3 shows the relationship between the absorbance of complex **4a** at $\lambda_{max} \cong 610$ nm and the microscopic solvent parameter $E_T(30)$.[15] The yield of complex **4a** increased with an increase in $E_T(30)$, indicating that polar solvents to favor the CT-complex formation[16] enhance the current efficiency for the

(15) (a) Reichardt, C. *Angew. Chem., Int. Ed. Engl.* **1979**, *18*, 98−110. (b) Zachariasse, K. A.; Phuc, N. V.; Kozankiewicz, B. *J. Phys. Chem.* **1981**, *85*, 2676−2683.

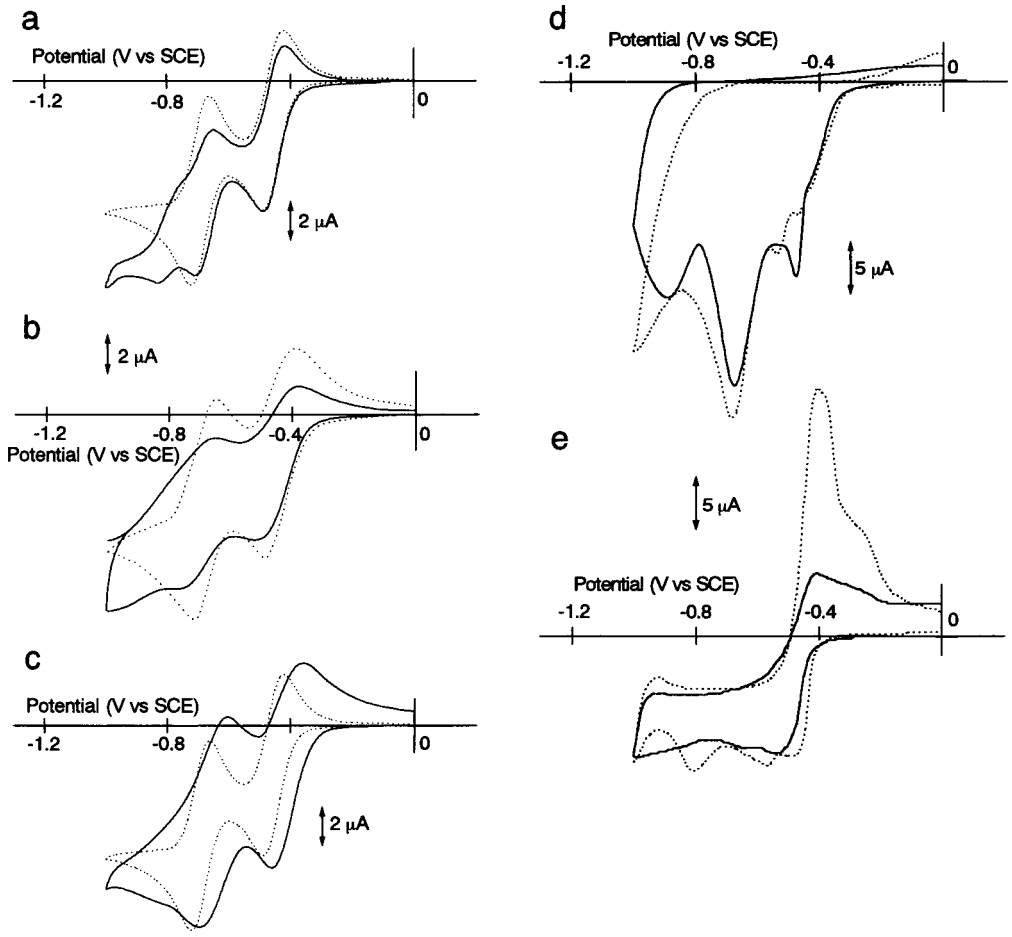

Figure 4. CVs of CH_3CN solutions containing Py (0.1 M), TNF (2 mM), and supporting electrolyte (0.1 M) at 20 °C (solid curves). Dotted curves show the voltammograms of CH_3CN solutions containing TNF (2 mM) and supporting electrolyte (0.1 M). Electrolyte: a, TEAP; b, TBAP; c, $TBABF_4$; d, $LiClO_4$; e, $NaClO_4$. Sweep rate: 20 mV/s. Working electrode: Pt disk (0.021 cm^2).

production of **4a** and supporting the essential role of the CT interaction. The solvent effect was also investigated previously regarding the chemical formation of Meisenheimer complexes in homogeneous reaction systems. Use of dipolar aprotic solvents such as dimethyl sulfoxide (DMSO) resulted in an increase and a decrease in the reaction constants of their formation and decomposition, respectively.[17] The effect was explained thermodynamically in terms of relative differences in stabilization of the reactants, complexes, and respective transition states, whereas in our electrochemical heterogeneous reaction systems, the solvent effect can be explained kinetically as an enhancement of the production rate of complex **4a** with the polarity of the solvent. The rate (i.e., the current flowing during the controlled-potential electrolysis) is proportional to the current efficiency for the reduction of the CT complex and hence is dependent on its equilibrium concentration. As described later, complex **4a** decomposes thermally. Use of such higher boiling solvents as DMF accelerated the decomposition to a greater extent during their evaporation and led to a lower isolation yield.

Salt Effect for the Formation of 4a. Because of the anionic character of complex **4**, the synthetic or electrode behavior should be affected by the cationic species of supporting electrolyte, and thus its effect was investigated by cyclic voltammetry. Figure 4 shows the CVs of CH_3CN solutions containing the mixture of Py (0.1 M)/TNF (2 mM) (solid curves) and TNF (2 mM) (dotted curves) in the presence of 0.1 M of TEAP (a), TBAP (b), $TBABF_4$ (c), $LiClO_4$ (d), and $NaClO_4$ (e). The solid curves of the CVs a−c show three redox waves identified as above. At the fixed electrode potential of −1.0 V, the green complex **4a** was formed in these cases. Use of $LiClO_4$ complicated the redox behavior of the mixture and TNF (Figure 4d) probably because of the insoluble nature of their two reduced forms: Large non-diffusion-controlled reduction peaks and no oxidation current upon scan reversal were observed. The second scan also showed no current response. When the potential was fixed at −1.0 V, the electrode surface was covered with an insoluble dull-red film, which is most likely identified as a lithium salt of **6**. The unsuccessful synthesis of complex **4a** may be due to the insulating nature of the film. The adsorption of a dull-red film also occurred during the reduction of TNF in a $NaClO_4$ electrolyte solution (dotted curve in Figure 4e), but it was reoxidized and decolorized at −0.4 V on the reverse scan. The shape of the CV waves for the mixture appears to be simple (solid curve), but its redox behavior approximates that for $LiClO_4$. The electrochemistry of

(16) Based on the CT theory, CT interaction increases with an increase in the solvent polarity: Turro, N. J. *Modern Molecular Photochemistry*; The Benjamin/Cummings Publishing: Menlo Park, CA, 1978; pp 136 and 137.

(17) (a) Larsen, J. W.; Amin, K.; Fendler, J. H. *J. Am. Chem. Soc.* **1971**, *93*, 2910−2913. (b) Fendler, J. H.; Larsen, J. W. *J. Org. Chem.* **1972**, *37*, 2608−2611. (c) Larsen, J. W.; Amin, K.; Ewing, S.; Magid, L. L. *J. Org. Chem.* **1972**, *37*, 3857−3860.

adsorption coupled with redox reactions may be far from simple, and the full accounting for the waves in parts d and e of Figure 4 is not clear yet. These results indicate that hydrophobic TEA^+ and TBA^+ cations give rise to stabilization of the electrogenerated anionic species, preventing their precipitation on the electrode surface and allowing the production of complex **4a**.

In homogeneous reaction systems, salt effects on the σ-complex formation have been reported. For example, Crampton and Khan[18] investigated the formation of a 1,1-dimethoxy complex by the reaction of 4-(methoxycarbonyl)-2,6-dinitroanisole with $CH_3O^-M^+$ ($M^+ = Li^+$, Na^+, K^+, and TBA^+). They showed that the complex anion is stabilized by ion-pair formation to a greater extent than CH_3O^- (the stabilization order $M^+ = K^+ > Na^+ > TBA^+$), while the effect is reversed with $M^+ = Li^+$. Micellar catalysis reported by Fendler et al.[19] is also an intriguing example of the salt effect on the σ-complex formation. In our heterogeneous system also, the ion pairing might be effective for enhancement of the rate of σ-complex formation, but the effect appears to be overshadowed by the hydrophobic−hydrophilic nature of the salt cation.

Role of O_2 in the Formation of 4 (Step 4). As described in the Experimental Section, all of the electrochemical experiments have been conducted under a flow of N_2 over the electrolyte solutions. However, oxygen gradually penetrated into the main compartment of the cell through the sintered glass frit (evidence for the penetration of O_2 is available in the Supporting Information), and accordingly, its effect would be pronounced during a long period of electrolysis. To investigate the contribution of O_2 to the synthesis of complex **4a**, in situ UV−vis absorption measurements were carried out during the controlled-potential electrolyses of the CH_3CN solution containing Py (2 mM), TNF (0.13 mM), and TEAP (0.1 M) at −1.0 V under a flow of N_2 (condition 1) and continuous bubbling of N_2 (condition 2). Figure 5 shows the variation in the UV−vis spectrum of the solution with electrolysis time (t) under conditions 1 and 2. Under condition 1, absorptions at $\lambda_{max} =$ 470 nm and in the near-IR region increased with t below $t \cong 60$ min, which is accompanied by a color change of the solution from orange (complex **1**) to red (complex **3**). Beyond $t \cong 60$ min, a new absorption at $\lambda_{max} = 610$ nm appeared and increased with t. This was accompanied by a decrease in the absorptions above 700 nm, giving rise to an isosbectic point at 700 nm. The color of the solution turned green (**4a**) from red (**3**). On the other hand, a time-dependent monotonic increase in absorptions at 470 nm and in the near-IR region was observed under condition 2; a color change from orange (**1**) to red (**3**) occurred during the electrolysis, and the resulting red solution immediately turned green upon exposure to air. These results demonstrate the crucial role of O_2 in the conversion of **3** into **4**. Considering the chemical reactivitiy of O_2 as a radical scavenger[20] and the chemical structure of **4a**,

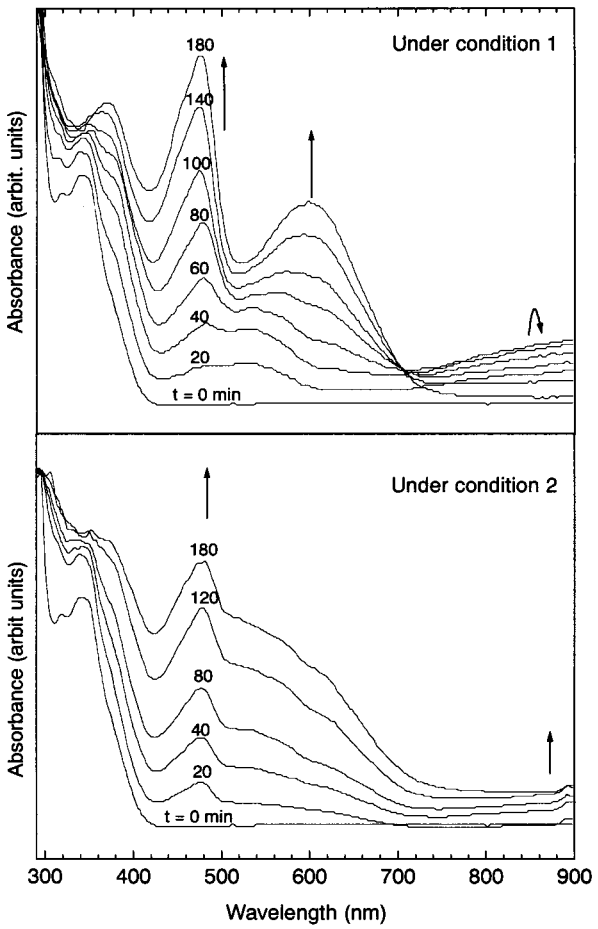

Figure 5. In situ absorption spectra of the mixture of Py (2 mM), TNF (0.13 mM), and TEAP (0.1 M) in CH_3CN during its bulk electrolysis (−1.0 V vs SCE) with stirring at 0 °C. The upper figure shows a change in the spectral shape with electrolysis time, t, under a flow of N_2 (condition 1) and the lower that under continuous bubbling of N_2 (condition 2).

attack of O_2 on the hydrogen atom of an activated Py with radical character as in complex **3** may cause collapse into the anionic complex **4** and a hydroperoxide anion (step 4).

Thermal Stability of Complex 4. Complex **4a** was stable at 0 °C and showed no decomposition in the solid state and in limited solvents such as acetone and CH_3CN. Time (t)-dependent changes in the UV−vis absorption maxima ($\lambda_{max} =$ 477 and 611 nm) of its acetone solution are shown in Figure 6a: The half-lives ($t_{1/2}$) were 20 and 5 h at 20 and 40 °C, respectively. Alternate use of DMSO and methanol (MeOH) showed $t_{1/2}$'s of 10 and 4 h at 20 °C, respectively (Figure 6b). A yellow solution was obtained when a green CH_3CN solution containing complex **4a** was allowed to stand at 20 °C for 1 week. The CV of the resulting yellow solution was the same in shape and position of the peaks as that of TNF (see dotted curve in Figure 4a). Additionally, controlled-potential bulk electrolysis of a CH_2Cl_2 solution containing complex **4a** and TEAP at 1.1 V under an N_2 atmosphere gave a black film (polypyrrole)[6] on a working Pt or an ITO (indium−tin oxide coated glass) plate electrode; when this electrolysis was prolonged until the end of polymerization reaction, a yellow

(18) (a) Crampton, M. R.; Khan, H. A. *J. Chem. Soc., Perkin Trans. 2* **1972**, 2286−2289. (b) Crampton, M. R. *J. Chem. Soc., Perkin Trans. 2* **1975**, 825 and 826.

(19) (a) Casilio, L. M.; Fendler, E. J.; Fendler, J. H. *J. Chem. Soc. B* **1971**, 1377−1380. (b) Fendler, E. J.; Fendler, J. H. *Chem. Commun.* **1970**, 816 and 817. (c) Fendler, J. H.; Fendler, E. J. Merritt, M. V. *J. Org. Chem.* **1971**, *36*, 2172−2176.

(20) Curran, D. P. In *Comprehensive Organic Synthesis*; Trost, B. M., Fleming, I., Eds.; Pergamon Press: Oxford, 1984; Vol. 4, p 715.

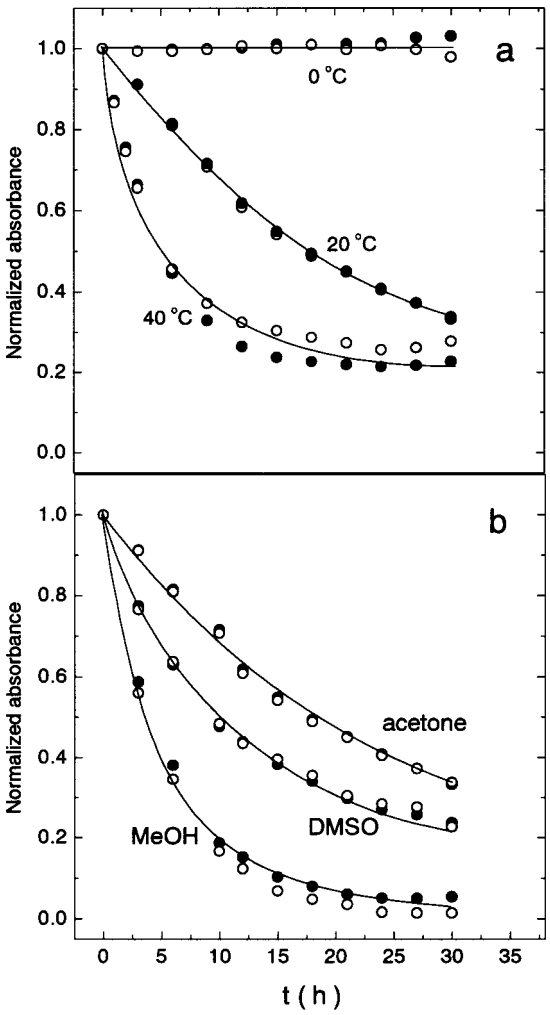

Figure 6. Degradation behavior of complex **4a**. The upper figure (a) shows the time (*t*)-dependent changes in the normalized absorbances of its acetone solution at 0, 20, and 40 °C. The lower figure (b) stands for the changes in acetone, DMSO, and MeOH at 20 °C. Open and closed circles indicate absorbances at ca. 610 and 477 nm, respectively.

solution was also produced and its CV waves were again in good agreement with those of TNF measured in a CH_2Cl_2/TEAP solution. These spectroscopic and electrochemical measurements indicate that complex **4a** decomposes thermally to give TNF as one of the products. The curves in Figure 6a obeyed good first-order kinetics, and the decomposition rate constants (k) were calculated to be 1.0×10^{-5} and 3.5×10^{-5} s^{-1} at 20 and 40 °C, respectively. Substituting these values in the Arrhenius equation yields an activation energy for the thermal decomposition, 64 kJ/mol. Of particular importance are the small values of k. The decomposition rate constant of most Meisenheimer complexes is in the wide range of $10^{8}-10^{-6}$ s^{-1}.[2c,d,21] Terrier el al. reported the most stable 4,6-dinitrobenzofuroxan complex with $k = 6.5 \times 10^{-9}$ s^{-1} in $H_2O/(CH_3)_2SO$ (1:1) at 20 °C and explained its unique stability in terms of the high activation energy for the decomposition (92 kJ/mol).[22] The k values of complex **4a** are close to the smallest

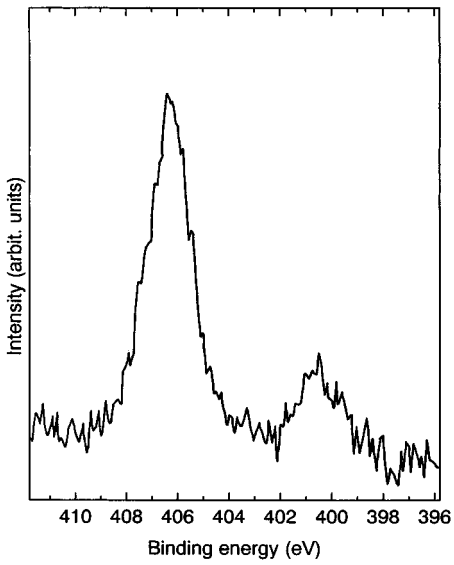

Figure 7. XPS spectrum in the N 1s region for the cast film of **4a**. The film was prepared on an ITO-coated glass plate.

limit of this range and therefore demonstrate it to be very stable. More importantly, higher stability was exhibited by complexes **4b** and **4c**, which decomposed with $k = 2.3 \times 10^{-6}$ and 4.8×10^{-6} s^{-1} at $\lambda_{max} \cong$ 610 nm in acetone at 20 °C, respectively. However, the high susceptibility of **4b** and **4c** to H^+-catalyzed decomposition[22a,23] prevented their purification by SiO_2 column chromatography and their isolation. This fits well the fact that Ind is more prone to C protonation than Py.

Electronic Structure of Complex 4a. To probe the electronic perturbation caused by the C−N bonding in complex **4a**, an XPS spectrum was taken of the N 1s core level region. The N 1s spectrum is shown in Figure 7 for a solution-cast film of complex **4a**. Nitrogen features centered at 406.3 and 400.4 eV were observed which can be assigned to the NO_2 group and pyrrolyl N 1s signals, respectively. The position of the N 1s signal of the Py monomer is reported to be 399.6 eV.[24] Based on an empirical relation of ∼5.8 eV binding energy shift per unit charge for the N 1s core level,[24a,25] the shift indicates that a charge of $\sim+1/7$ is induced on the pyrrolyl nitrogen atom in complex **4a** compared to the monomeric Py nitrogen. This electronic structure is consistent with the results of theoretical calculations by Caveng et al.[26] They showed that, despite the negative charge of the Meisenheimer complex, its carbon framework is electron-deficient because the electrons are mostly attracted by the nitro group. The displacement of the charge in complex **4a** may be explained on this basis. In addition, the large binding energy of the NO_2 group in complex **4a**, 406.3 eV, is worthy of remark: Nitrogen species with a binding energy above 406 eV are limited to NO_3^-, a nitroxy group, N_2O and

(21) Bernasconi, C. F. *J. Am. Chem. Soc.* **1968**, *90*, 4982−4988.
(22) (a) Terrier, F.; Millot, F.; Norris, W. P. *J. Am. Chem. Soc.* **1976**, *98*, 5883−5890. (b) Terrier, F.; Sorkhabi, H. A.; Millot, F.; Halle, J. C.; Schaal, R. *Can. J. Chem.* **1980**, *58*, 1155−1160.
(23) Terrier, F.; Millot, F.; Chatrousse, A. P.; Yagupolskii, L. M.; Boiko, V. N.; Shchupak, G. M.; Ignatev, N. V. *J. Chem. Res. (S)* **1979**, 272 and 273.
(24) (a) Pfluger, P.; Street, G. B. *J. Chem. Phys.* **1984**, *80*, 544−553. (b) Clark, D. T.; Lilley, D. M. J. *Chem. Phys. Lett.* **1971**, *9*, 234−237.
(25) Pfluger, P.; Krounbi, M.; Street, G. B. *J. Chem. Phys.* **1983**, *78*, 3212−3218.
(26) Caveng, P.; Fischer, P. B.; Heilbronner, E.; Miller, A. L.; Zollinger, H. *Helv. Chim. Acta* **1967**, *50*, 848−860.

NO adsorbed on aluminum, and metal-coordinated ligands such as NO_3, ONO_2, and nitrophenyl.[25,27]

The cast film of complex **4a** possesses a smooth, pinhole-free surface. This surface property, along with the unique electron-transporting property of the TNF moiety[5] and the stability of its radical character, enabled us to measure the electrical conductivity of the film. The film was prepared by dipping an ITO plate in an acetone solution of **4a**. After drying and evaporation of an Au electrode (area 0.28 cm^2) on the top of the film (thickness 1.4 μm), the current−voltage ($J-V$) measurement was carried out in a sealed box using a digital multimeter (Advantest R8240). The series of experimental procedures described above, i.e., dipping → drying → vacuum evaporation of the Au electrode → $J-V$ measurement, was performed without a break in order to minimize decomposition of complex **4a**. The $J-V$ plot gave a straight line intersecting the origin. The conductivity of 2.9×10^{-5} S cm^{-1} was calculated from the slope of the plot. This value is grouped among the semiconductors[28] and is relatively high despite the weak interaction between the molecules in the amorphous organic solid, which is undoubtedly due to the ability of radical species to conduct electrical current. These results suggest that our novel electrochemical route gives Meisenheimer complexes with unique electronic as well as chemical structures.

Concluding Remarks

A mechanistic study on the electrochemical formation of Meisenheimer complexes has been done. Experimental evidence revealed that the complexes are distinct from the earlier ones in that their formation is initiated by the electrode reduction and completed by the attack of O_2. We believe this route opens a new avenue in nucleophilic aromatic substitution reactions because it might be another route to Meisenheimer complexes. Additionally, their high stability and unique electronic structure would also be notable features. Studies to characterize their polymerization behavior are underway, and we are also beginning to explore the structural and electronic properties of the resulting conducting films of polypyrrole, polyindole, and polycarbazole.

Acknowledgment. The authors thank T. Sibuya of Idemitsu Kosan Co. for help with the XPS analyses. This work was partially supported by a grant from the Futaba Memorial Foundation, Japan.

Supporting Information Available: Cyclic voltammograms of a Py−TNF mixture at sweep rates of 10−200 mV/s, evidence for the penetration of O_2, and calculated UV−vis electronic spectra for the isomers of **4a** (PDF). This material is available free of charge via the Internet at http://pubs.acs.org.

CM010488I

(27) (a) Hendrickson, D. N.; Hollander, J. M.; Jolly, W. *Inorg. Chem.* **1969**, *8*, 2042−2047. (b) Burger, K.; Tschismarov, F.; Ebel, H. *J. Electron Spectrosc. Relat. Phenom.* **1977**, *10*, 461−465. (c) Wagner, C. D.; Riggs, W. H.; Davis, L. E.; Moulder, J. F. In *Handbook of X-ray Photoelectron Spectroscopy*; Muilenberg, G. E., Ed.; Perkin-Elmer: Eden Prairie, MN, 1979; pp 38 and 39. (d) Wagner, C. D.; Naumkin, A. V.; Kraut-Vass, A.; Allison, J. W.; Powell, C. J.; Rumble, J. R., Jr.; Lee, A. Y.; Blakeslee, D. M. *NIST X-ray Photoelectron Spectroscopy Database (NIST Standard Reference Database 2.0*, Version 3.0 (web version)); NIST: Gaithersburg, MD, 2001.

(28) Callister, W. D., Jr. *Materials Science and Engineering—An Introduction*; John Wiley & Sons: New York, 1994; Chapter 19, pp 591 and 592.